ELSEVIER

Engineering Analysis with Boundary Elements 28 (2004) 1387–1403

ENGINEERING ANALYSIS *with* BOUNDARY ELEMENTS

www.elsevier.com/locate/enganabound

Highly accurate solutions of Motz's and the cracked beam problems

T.T. Lu, H.Y. Hu, Z.C. Li*

Department of Applied Mathematics and Department of Computer Science and Engineering, National Sun Yat-Sen University, Kaohsiung 80424, Taiwan, ROC

Received 17 June 2003; revised 30 January 2004; accepted 21 March 2004

Available online 13 July 2004

Abstract

For Motz's problem and the cracked beam problem, the collocation Trefftz method is used to seek their approximate solutions $u_N = \sum_{i=0}^{N} D_i r^{i+(1/2)} \cos(i+(1/2))\theta$, where D_i are the expansion coefficients. The high-order Gaussian rules and the central rule are used in the algorithms, to link the collocation method and the least squares method, and to provide exponential convergence rates of the obtained solutions. Compared with the solutions in the previous literature, our Motz's solutions are more accurate and the leading coefficient D_0 using the Gaussian rule with six nodes arrives at 17 significant (decimal) digits. Similarly for the cracked beam problem, the collocation Trefftz method also provides the highly accurate solutions, and D_0 with 17 significant digits by the Gaussian rules. This papers proves that when the rules of quadrature involved have the relative errors less than three quarters, the solution form the collocation Trefftz method may converge exponentially. Such an analysis supports the collocation Trefftz method to become theoretically the most accurate method for Motz's and the cracked beam problems.

Keywords: Collocation Trefftz method; Boundary approximation method; Least squares method; Gaussian quadrature; Motz's problem; Cracked beam problem; Singularity problems; Highly accurate solutions

1. Introduction

Motz's problem was first discussed by Motz [18] in 1947 for the relaxation method. Since then, many researchers have selected Motz's problem as a prototype of singularity problems for verifying efficiency of numerical methods [14]. Motz's problem solves the Laplace equation on the rectangle $S = \{(x,y) | -1 < x < 1, 0 < y < 1\}$

$$\Delta u = \frac{\partial^2 u}{\partial x^2} + \frac{\partial^2 u}{\partial y^2} = 0, \text{ in } S, \tag{1.1}$$

with the mixed Neumann–Dirichlet boundary conditions, Fig. 1

$$u|_{x<0 \wedge y=0} = 0, \qquad u|_{x=1} = 500, \tag{1.2}$$

$$\left.\frac{\partial u}{\partial y}\right|_{y=1} = \left.\frac{\partial u}{\partial y}\right|_{x>0 \wedge y=0} = \left.\frac{\partial u}{\partial x}\right|_{x=-1} = 0. \tag{1.3}$$

Note that there exists a singularity at the origin (0,0) due to the intersection of the Neumann–Dirichlet boundary conditions. In fact, the singular solutions of Eqs. (1.1)–(1.3) are found as

$$u(r,\theta) = \sum_{i=0}^{\infty} d_i r^{i+(1/2)} \cos\left(i + \frac{1}{2}\right)\theta, \tag{1.4}$$

where d_i is the true expansion coefficient, and (r,θ) are the polar coordinates with the origin at (0,0) (Fig. 1). Since its convergence radius, $R = 2$, is analyzed in Ref. [20], the series expansions (1.4) are well suited to the entire solution domain S. Hence, the admissible functions with finite terms

$$u_N(r,\theta) = \sum_{i=0}^{N} D_i r^{(i+(1/2))} \cos\left(i + \frac{1}{2}\right)\theta, \tag{1.5}$$

where D_i the unknown coefficients, are most efficient as numerical Motz's solutions. The exponential convergence rates $O(e^{-cN})$ can be obtained for Eq. (1.5) with some positive constant c. When function (1.5) is chosen, Eq. (1.1), $u|_{x<0\wedge y=0}$ and $\partial u/\partial y|_{x>0\wedge y=0}$ are satisfied automatically. Then the coefficients D_i are sought by the collocation equations of the rest boundary conditions in Eqs. (1.2) and (1.3). This is called the boundary approximation method (BAM) in Refs. [14,16] or the collocation Trefftz method in this paper. Under the computation in double precision and $N = 34$, the maximal absolute error at $x = 1$ (e.g. on $\overline{AB}$) of

* Corresponding author.
E-mail address: zcli@math.nsysu.edu.tw (Z.C. Li).

0955-7997/$ - see front matter © 2004 Elsevier Ltd. All rights reserved.
doi:10.1016/j.enganabound.2004.03.005

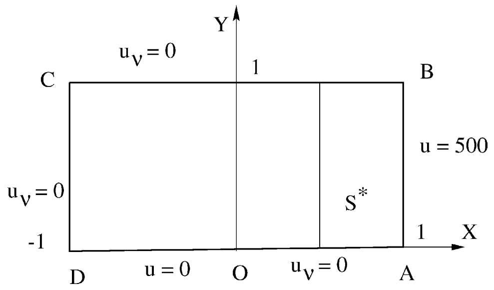

Fig. 1. Motz's problem.

the Motz's solution in Ref. [16] reaches up to 5.47×10^{-9}. Also the leading coefficient D_0 in Ref. [16] has 12 significant digits. The solutions in Ref. [16] have been recognized to be the very accurate solutions for Motz's problem [5,6,17]. In this paper, to pursue the better leading coefficient D_0, we choose the Gaussian rules of high orders. Surprisingly, the obtained D_0 may have 17 significant digits by Fortran programs in double precision. Based on the new results in this paper, we may address that the collocation Trefftz method (i.e. the BAM) is the highly accurate method for Motz's problem, not only in the global solutions but also in the leading coefficient D_0. As for Motz's problem, the conformal transformation method of Rosser and Papamichael [20] can also yield the most accurate leading coefficient D_0.

The same approaches are applied to the cracked beam problem, which is another frequently used model for testing new numerical methods [4–6,19,21]. Its highly accurate solutions are also provided with the leading D_0 having 17 significant digits. The advantage of the cracked beam problem over Motz's problem is that half of the expansion coefficients are zero.

This paper is organized as follows. In Section 2, basic algorithms of the collocation Trefftz method are provided for Motz's problem, and the highly accurate solutions are obtained in double precision. In Section 3, a new analysis is made for the quadrature involved. In Section 4, the cracked beam problem is discussed, and its highly accurate solutions and the leading coefficient D_0 with 17 significant digits are also reported. In Section 5, some discussions and comparisons are made, and in Section 6, concluding remarks are addressed.

2. Basic algorithms of collocation Trefftz method

Since the expansion (1.5) satisfies the Laplace equation and boundary conditions at $y = 0$, the coefficients D_i should be chosen to satisfy the rest of the boundary conditions

$$u|_{x=1} = u|_{\overline{AB}} = 500, \tag{2.1}$$

$$\left.\frac{\partial u}{\partial y}\right|_{y=1} = \left.\frac{\partial u}{\partial \nu}\right|_{\overline{BC}} = 0, \qquad \left.\frac{\partial u}{\partial \nu}\right|_{x=-1} = -\left.\frac{\partial u}{\partial x}\right|_{\overline{CD}} = 0, \tag{2.2}$$

as best as possible, where $u_\nu = \partial u/\partial \nu$ is the outward normal derivative to ∂S, and $\overline{AB}$, $\overline{BC}$ and $\overline{CD}$ are shown in Fig. 1. Hence, the least squares method (LSM) may be designed as follows. Denote

$$[u, v] = \int_{\overline{AB}} uv \, dl + w^2 \int_{\overline{BC} \cup \overline{CD}} u_\nu v_\nu \, dl, \tag{2.3}$$

where w is a positive weight constant, and a good choice of the weight

$$w = \frac{1}{N+1}, \tag{2.4}$$

can be found in Ref. [16]. Denote by V_N the collection of finite dimensional function (1.5). Then, we may seek $u_N \in V_N$ such that

$$[u_N, v] = (f, v), \quad \forall v \in V_N, \tag{2.5}$$

where

$$(f, v) = 500 \int_{\overline{AB}} v \, dl. \tag{2.6}$$

Denote the energy

$$I(v) = \int_{\overline{AB}} (v - 500)^2 \, dl + w^2 \int_{\overline{BC} \cup \overline{CD}} v_\nu^2 \, dl. \tag{2.7}$$

The solution of Eq. (2.5) can also be expressed by: to seek $u_N \in V_N$ such that

$$I(u_N) = \min_{v \in V_N} I(v). \tag{2.8}$$

Both Eqs. (2.5) and (2.8) lead to the same linear algebraic system

$$\mathbf{A}\vec{x} = \vec{b}, \tag{2.9}$$

where $\vec{x} \in R^{N+1}$ is the unknown vector consisting of coefficients D_i, $i = 0, \ldots, N$, and $\vec{b} \in R^{N+1}$ is the known vector resulting from the non-homogeneous Dirichlet condition (2.1), and the associate matrix, $\mathbf{A} \in R^{(N+1)\times(N+1)}$, is symmetric positive definite, but not sparse. By the Gaussian elimination without pivoting in Ref. [7], the coefficients D_i (i.e. $\vec{x}$) can be obtained. Once the coefficients D_i are known, the errors on $\overline{AB} \cup \overline{BC} \cup \overline{CD}$

$$\|u - u_N\|_B = \left[\int_{\overline{AB}} (500 - u_N)^2 dl + w^2 \int_{\overline{BC} \cup \overline{CD}} (u_N)_\nu^2 dl \right]^{1/2} = \sqrt{I(u_N)} \tag{2.10}$$

are computable, where the notation is

$$\|v\|_B = \sqrt{[v, v]}. \tag{2.11}$$

Suppose that certain rules of integration are adopted to the integrals in Eq. (2.7). Let $\overline{AB}$ be divided into small segments

$\overline{Z_iZ_{i+1}}$, i.e. $\overline{AB} = \bigcup_i \overline{Z_iZ_{i+1}}$. Then the integral is evaluated by some rules

$$\int_{\overline{AB}} v^2 \, dl \approx \tilde{\int}_{\overline{AB}} v^2 \, dl = \sum_i \tilde{\int}_{\overline{Z_iZ_{i+1}}} v^2 \, dl. \tag{2.12}$$

For example, the central and trapezoidal rules are given by

$$\tilde{\int}_{\overline{Z_iZ_{i+1}}} v^2 \, dl = v_{i+(1/2)}^2 h_i, \tag{2.13}$$

and

$$\tilde{\int}_{\overline{Z_iZ_{i+1}}} v^2 \, dl = \frac{1}{2}(v_i^2 + v_{i+1}^2)h_i, \tag{2.14}$$

respectively, where $h_i = \overline{Z_iZ_{i+1}}$, $v_i = v(Z_i)$, $v_{i+(1/2)} = v(Z_{i+(1/2)})$ and $Z_{i+(1/2)} = Z_i + Z_{i+1}/2$. Other kinds of Newton–Cotes and Gaussian rules can also be employed and will be discussed later. Hence, for the numerical quadrature, we may seek $\tilde{u}_N \in V_N$ such that

$$\tilde{I}(\tilde{u}_N) = \min_{v \in V_N} \tilde{I}(v), \tag{2.15}$$

where

$$\tilde{I}(v) = \tilde{\int}_{\overline{AB}} (v - 500)^2 dl + w^2 \tilde{\int}_{\overline{BC} \cup \overline{CD}} v_\nu^2 \, dl. \tag{2.16}$$

The minimization of $\tilde{I}(v)$ also leads to a linear system like Eq. (2.9). This is a direct implementation to the LSM involving numerical integration, called the normal method.

Now, we turn to the collocation Trefftz method, which can be regarded as a certain kind of the LSM involving specific quadratures. For simplicity in exposition, let us first consider the central rule (2.13). Divide the boundary $\overline{AB}$, $\overline{BC}$ and $\overline{CD}$ into uniform sub-intervals (Fig. 1). Then

$$h = \frac{\overline{AB}}{M} = \frac{\overline{CD}}{M} = \frac{\overline{CB}}{2M}. \tag{2.17}$$

Eqs. (2.1) and (2.2) can be transformed to the boundary collocation equations

$$u_N(P_i) = 500, \qquad i = 1, 2, \ldots, M, \tag{2.18}$$

$$\frac{\partial u_N}{\partial x}(P_i^*) = -\frac{\partial u_N}{\partial \nu}(P_i^*) = 0, \qquad i = 1, 2, \ldots, M, \tag{2.19}$$

$$\frac{\partial u_N}{\partial y}(Q_i^\pm) = \frac{\partial u_N}{\partial \nu}(Q_i^\pm) = 0, \qquad i = 1, 2, \ldots, M. \tag{2.20}$$

Let $x_i^\pm = \pm(i - (1/2))h$ and $y_i = (i - (1/2))h$. The nodes $P_i = (1, y_i) \in \overline{AB}$, $P_i^* = (-1, y_i) \in \overline{CD}$ and $Q_i^\pm = (x_i^\pm, 1) \in \overline{BC}$, and their polar coordinates are computed by

$$P_i = (r_i, \theta_i), \quad r_i = \sqrt{1 + y_i}, \quad \theta_i = \cos^{-1}\left(\frac{1}{\sqrt{1 + y_i^2}}\right),$$

$$P_i^* = (r_i, \theta_i^*), \qquad \theta_i^* = \pi - \theta_i,$$

where $0 < \theta_i < \pi/2$. Besides

$$Q_i^\pm = (\bar{r}_i, \theta_i^\pm), \qquad \bar{r}_i = \sqrt{1 + x_i^2},$$

$$\theta_i^+ = \sin^{-1}\left(\frac{1}{\sqrt{1 + x_i^2}}\right),$$

where $0 < \theta_i^+ < \pi/2$ and $\theta_i^- = \pi - \theta_i^+$

In Eqs. (2.18)–(2.20), there are $m = 4M$ equations, but $N + 1$ unknown coefficients. Usually, select $m > N + 1$. We invoke the standard least squares method in Ref. [7] to solve the overdetermined system of Eqs. (2.18)–(2.20). Denote Eqs. (2.18)–(2.20) by

$$\mathbf{F}_i \vec{x} = \vec{b}_i, \qquad i = 1, 2, 3, \tag{2.21}$$

respectively, where $\mathbf{F}_i$ and $\vec{b}_i$ are the known matrices and vectors, respectively. Since Eq. (2.21) results from different boundary conditions, different weights should also be assigned. When the weights $\sqrt{h}$ and $w\sqrt{h}$ are applied to the first and the other two equations in Eq. (2.21), the global target function becomes

$$T(\vec{x}) = h\|\mathbf{F}_1\vec{x} - \vec{b}_1\|^2 + w^2 h \sum_{i=2}^{3} \|\mathbf{F}_i\vec{x} - \vec{b}_i\|^2, \tag{2.22}$$

where $\|\cdot\|$ is the Euclidean norm, and w is a suitable weight constant (Eq. (2.4)). We can easily verify the following lemma by direct manipulation.

Lemma 2.1. *Let the central rule* (2.13) *be used in* Eqs. (2.16) and (2.21) *be the collocation equations* (2.18)–(2.20). *Then we have*

$$\tilde{I}(\tilde{u}_N) = T(\vec{x}), \tag{2.23}$$

where $\tilde{I}(\tilde{u}_N)$ and $T(\vec{x})$ are defined in Eqs. (2.16) and (2.22), *respectively.*

Note that the admissible functions and their derivatives are given by

$$u_N = u_N(r, \theta) = \sum_{l=0}^{N} D_l r^{l+(1/2)} \cos\left(l + \frac{1}{2}\right)\theta,$$

$$\frac{\partial u_N}{\partial x} = \sum_{l=0}^{N} D_l \left(l + \frac{1}{2}\right) r^{l-(1/2)} \cos\left(l - \frac{1}{2}\right)\theta,$$

$$\frac{\partial u_N}{\partial y} = \sum_{l=0}^{N} D_l \left(l + \frac{1}{2}\right) r^{l-(1/2)} \sin\left(\frac{1}{2} - l\right)\theta. \tag{2.24}$$

Then, Lemma 2.1 enables us to obtain the solutions D_i by solving the following overdetermined system of the equations

$$\sqrt{h}\sum_{l=0}^{N} D_l r_i^{l+(1/2)}\cos\left(l+\frac{1}{2}\right)\theta_i = \sqrt{h}500, \qquad 1 \le i \le M, \tag{2.25}$$

$$w\sqrt{h}\sum_{l=0}^{N} D_l\left(l+\frac{1}{2}\right)(r_i)^{l-(1/2)}\cos\left(l-\frac{1}{2}\right)\theta_i^* = 0,$$
$$\theta_i^* = \pi - \theta_i, \qquad 1 \le i \le M, \tag{2.26}$$

$$w\sqrt{h}\sum_{l=0}^{N} D_l\left(i+\frac{1}{2}\right)(\bar{r}_i)^{l-(1/2)}\sin\left(\frac{1}{2}-l\right)\theta_i^{\pm} = 0,$$
$$\theta_i^- = \pi - \theta_i^+, \qquad 1 \le i \le M, \tag{2.27}$$

where $m = 4M > N+1$. Denote the overdetermined system of Eqs. (2.25)–(2.27) by

$$\mathbf{F}\vec{x} = \vec{b}^*, \tag{2.28}$$

where the associated matrix $\mathbf{F} \in R^{m\times(N+1)}$, $\vec{b}^* \in R^m$ and $\vec{x} \in R^{N+1}$. In fact, the entries of $\mathbf{F} = (F_{il})$ are given by

The Gaussian rules with r nodes are given by

$$\int_{-1}^{1} f(t)\mathrm{d}t \approx \tilde{\int}_{-1}^{1} f(t)\mathrm{d}t = \int_{-1}^{1} \hat{f}(t)\mathrm{d}t = \sum_{i=1}^{r} \omega_i f(t_i), \tag{2.34}$$

where the locations of nodes $t_i \in [-1,1]$ and positive weights ω_i are provided in textbooks [1]. For Eq. (2.30), a point P_i located at the jth node of $\overline{Z_k Z_{k+1}} \in \overline{AB}$ has the weights $\alpha_i = \sqrt{\omega_j h_k/2}$. The weights β_i and γ_i can be obtained similarly. When $r=1$, the Gaussian rule is just the central rule with $t_1 = 0$ and $\omega_1 = 2$. For the Gaussian rules, we have the following proposition, similar to Lemma 2.1.

Proposition 2.1. *Let the Gaussian rules* (2.34) *be used in Eq.* (2.16), *and* $m \ge N+1$. *Then the coefficients* D_ℓ *from the corresponding collocation equations* (2.30)–(2.32) *are just the solutions from Eq.* (2.15).

Let us consider the computer complexity of this method. In Eq. (2.29) we may employ the recursive formulas to save CPU time:

$$F_{i,l} = \begin{cases} \sqrt{h} r_i^{l+(1/2)}\cos\left(l+\frac{1}{2}\right)\theta_i, & 1 \le i \le M,\ 0 \le l \le N, \\ w\sqrt{h}\left(l+\frac{1}{2}\right) r_{i-M}^{l-(1/2)}\cos\left(l-\frac{1}{2}\right)\theta_{i-M}^*, & M < i \le 2M,\ 0 \le l \le N, \\ w\sqrt{h}\left(l+\frac{1}{2}\right) \bar{r}_{i-2M}^{l-(1/2)}\sin\left(\frac{1}{2}-l\right)\theta_{i-2M}^+, & 2M < i \le 3M,\ 0 \le l \le N, \\ w\sqrt{h}\left(l+\frac{1}{2}\right) \bar{r}_{i-3M}^{l-(1/2)}\sin\left(\frac{1}{2}-l\right)\theta_{i-3M}^-, & 3M < i \le 4M,\ 0 \le l \le N. \end{cases} \tag{2.29}$$

In general, we can rewrite the overdetermined system of Eqs. (2.25)–(2.27) as

$$\alpha_i(u_N(P_i) - 500) = 0, \qquad P_i \in \overline{AB}, \tag{2.30}$$

$$w\beta_i \frac{\partial u_N}{\partial x}(P_i^*) = 0, \qquad P_i^* \in \overline{CD}, \tag{2.31}$$

$$w\gamma_i \frac{\partial u_N}{\partial y}(Q_i) = 0, \qquad Q_i \in \overline{BC}, \tag{2.32}$$

where P_i and P_i^* and Q_i are the nodes of integration rules, and α_i, β_i and γ_i are positive weights. Eqs. (2.30)–(2.32) may come from other quadratures. Take the Gaussian rules for example. Denote $h_k = \overline{Z_k Z_{k+1}}$. By using an affine transformation, the interval $[Z_k, Z_{k+1}]$ can be converted to $[-1,1]$. Hence by this transformation, $x \in \overline{Z_k Z_{k+1}}$ is mapped to $t \in [-1,1]$, $f(x)$ to $\hat{f}(t)$, and the integral on $\overline{Z_k Z_{k+1}}$ is changed to

$$\int_{\overline{Z_k Z_{k+1}}} f(x)\mathrm{d}x = \frac{h_k}{2}\int_{-1}^{1} \hat{f}(t)\mathrm{d}t. \tag{2.33}$$

$$\cos\left(l+\frac{1}{2}\right)\theta = 2\cos\theta\cos\left(l-\frac{1}{2}\right)\theta - \cos\left(l-\frac{3}{2}\right)\theta, \tag{2.35}$$
$$r_i^{l+(1/2)} = r_i r_i^{l-(1/2)}.$$

To solve the least squares solution of Eq. (2.28) with full rank $\mathbf{F}$, we may use the QR method by the Householder orthogonalization with the flops [7, p. 248]

$$T_L = 2mn^2 - \frac{2n^3}{3}, \qquad n = N+1. \tag{2.36}$$

On the other hand, the normal equations from Eq. (2.28) are

$$\mathbf{A}\vec{x} = \mathbf{F}^{\mathrm{T}}\mathbf{F}\vec{x} = \mathbf{F}^{\mathrm{T}}\vec{b}^* = \vec{b}, \tag{2.37}$$

where $\mathbf{A}$ is symmetric positive definite. Then the flops for $\mathbf{F}^{\mathrm{T}}\mathbf{F}$ and the Gaussian elimination of symmetric matrices are $m(n^2+n)$ and $(1/3)n^3$, respectively. So the main flops needed is

$$T_N = mn^2 + \frac{1}{3}n^3. \tag{2.38}$$

Table 1
The error norms and condition numbers from the collocation Trefftz method for Motz's problem by the central rule

N	M	$\|\varepsilon\|_B$	$\|\varepsilon\|_{\infty,\overline{AB}}$	Cond.	$\left\|\frac{\Delta D_0}{D_0}\right\|$	$\left\|\frac{\Delta D_1}{D_1}\right\|$	$\left\|\frac{\Delta D_2}{D_2}\right\|$	$\left\|\frac{\Delta D_3}{D_3}\right\|$
10	8	0.250(−1)	0.149(−1)	94.3	0.189(−5)	0.491(−5)	0.601(−5)	0.928(−3)
18	12	0.133(−3)	0.811(−4)	0.193(4)	0.158(−7)	0.113(−6)	0.290(−6)	0.502(−6)
26	16	0.973(−6)	0.734(−6)	0.366(5)	0.216(−9)	0.155(−8)	0.380(−8)	0.202(−8)
34	24	0.839(−8)	0.459(−8)	0.666(6)	0.169(−11)	0.121(−10)	0.296(−10)	0.152(−10)

In our case, $n=N+1$ and $m=4N$. Evidently, when $m \gg n$, we have $T_L \le 2T_N$, and when $m \ge n$

$$T_L - T_N = (m-n)n^2 \ge 0.$$

Then we conclude the following

Corollary 2.1. *The flops needed to solve a least squares problem* (2.28) *by the Householder QR method are larger than, but at most double of those by the normal method* (2.37).

Besides the QR method, the singular value decomposition (SVD) can also be used to solve the overdetermined system (2.28). A comparison between the QR method and the SVD is given in Ref. [3]. In general, the latter uses more flops than the former. So the SVD is not recommended here.

Since the condition number of matrix **A** is nearly square of that of matrix **F** [7], using the normal equations incurs a serious loss of solution accuracy for Motz's problem. Some numerical experiments of the normal method were reported in Lefeber [12], where only four and five significant digits of Motz's solutions were obtained from the computation in double precision. Hence to obtain the numerical solutions of Motz's problem, we always choose the QR method to solve Eq. (2.28). Such a numerical approach is called the BAM in Refs. [14,16] and the collocation Trefftz method in this paper.[1] Note that stability analysis of the collocation Trefftz method has been explored in Ref. [14].

To close this section, we provide numerical experiments for Motz's problem. First, for the central rule, errors of the solutions and condition numbers are listed in Tables 1 and 2, where $\varepsilon = u - u_N$, M denotes the number of collocation nodes along $\overline{AB}$, and the total number of all collocation nodes used is $4M$. In these tables, $\Delta D_i = d_i - D_i$, $\|\varepsilon\|_{0,\overline{AB}} = \max_{\overline{AB}} |\varepsilon|$, and the condition number is defined by

$$\text{Cond.} = \left\{ \frac{\lambda_{\max}(\mathbf{F}^{\mathrm{T}}\mathbf{F})}{\lambda_{\min}(\mathbf{F}^{\mathrm{T}}\mathbf{F})} \right\}^{1/2} = \left\{ \frac{\lambda_{\max}(\mathbf{A})}{\lambda_{\min}(\mathbf{A})} \right\}^{1/2},$$

where $\lambda_{\max}(\mathbf{A})$ and $\lambda_{\min}(\mathbf{A})$ are the maximal and minimal eigenvalues of **A**, respectively. It can be seen from Table 2 that M should be chosen as $M \ge N/2$ for $N = 34$. Tables 1–16 are all computed by means of Fortran programs in double precision.

Moreover, for the Gaussian rule with six nodes and those with 1, 2, 4, 6, 8 and 10 nodes, the results are listed in Tables 3 and 4, respectively, and the best leading coefficients in Table 5 by the Gaussian rule with six noes as $N = 34$ and $M = 30$. Note that the central rule is the simplest Gaussian rule with $r = 1$. When using the Gaussian rule, there seems no significant effect to reduce the errors $\|\varepsilon\|_B$ and $\|\varepsilon\|_{\infty,\overline{AB}}$ (e.g. from $\|\varepsilon\|_B = 0.839(-8)$ down to 0.428(−8), Table 4). From Table 4, however, the Gaussian rules of high order do improve evidently the accuracy of leading coefficients. For $N = 34$, $M = 30$, and the Gaussian rule of six nodes, the highly accurate solutions are listed in Table 5 with the best leading coefficient

$$D_0 = 401.162453745234416. \tag{2.39}$$

Compared this D_0 in Eq. (2.39) with more accurate values [14,15] using Mathematica, the relative error is less than the rounding error of double precision![2] Note that D_0 in Eq. (2.39) has 17 significant decimal digits; while the D_0 in Refs. [14,16] has only 12 significant digits. This is an important evolution of Refs. [14,16]. Besides, we also list D_i with significant digits (Sig. digits) in Table 5, which are obtained from D_i with all digits by rounding. The errors of Sig digits occur only at the last digit at most with a half unit, compared with the more accurate coefficients in Ref. [15]. Although $D_{28} - D_{34}$ are incorrect, they are indispensable to reach the global optimal solutions. Hence, the solutions from this paper are optimal in the global errors,

[1] Strictly speaking, the description of BAM in Refs. [14,16] does not involve numerical quadrature; the computed results in Refs. [14,16] are obtained by the algorithms described in this paper using the central rule. The BAM involving numerical integration leads to the collocation Trefftz method. We join the BAM into the Trefftz family recently for easy communication with others.

[2] This seems impossible! In fact, there exist some guard digits in computer for arithmetic of floating point numbers by noting that there are 18 digits in computer outputs of double precision, and some cancellation of rounding errors in statistics may also happen in the computation. Hence, this occasionally excellent results may happen in random, which have been caught carefully by our computation and provided in Tables 5, 12 and 15. However, we can see from Table 4 that coefficient D_0 has at least 16 significant digits by the Gaussian rule with high order.

Table 2
The error norms and condition numbers from the collocation Trefftz method for Motz's problem by the central rule as $N = 34$

M	$\|\varepsilon\|_B$	$\|\varepsilon\|_{\infty,\overline{AB}}$	Cond.	$\left\|\frac{\Delta D_0}{D_0}\right\|$	$\left\|\frac{\Delta D_1}{D_1}\right\|$	$\left\|\frac{\Delta D_2}{D_2}\right\|$	$\left\|\frac{\Delta D_3}{D_3}\right\|$
9	0.135(−8)	0.496(−6)	0.267(8)	0.377(−9)	0.266(−8)	0.641(−8)	0.342(−8)
12	0.587(−8)	0.713(−7)	0.992(6)	0.337(−10)	0.239(−9)	0.578(−9)	0.305(−9)
16	0.772(−8)	0.189(−7)	0.679(6)	0.729(−11)	0.520(−10)	0.127(−9)	0.655(−10)
24	0.839(−8)	0.459(−8)	0.669(6)	0.169(−11)	0.121(−11)	0.296(−10)	0.152(−10)
32	0.849(−8)	0.462(−8)	0.669(6)	0.769(−11)	0.550(−11)	0.134(−10)	0.695(−11)

Table 3
The error norms and condition numbers from the collocation Trefftz method for Motz's problem as $N = 34$ by the Gaussian rule with six nodes

M	$\|\varepsilon\|_B$	$\|\varepsilon\|_{\infty,\overline{AB}}$	Cond.	$\left\|\frac{\Delta D_0}{D_0}\right\|$	$\left\|\frac{\Delta D_1}{D_1}\right\|$	$\left\|\frac{\Delta D_2}{D_2}\right\|$	$\left\|\frac{\Delta D_3}{D_3}\right\|$
12	0.359(−8)	0.721(−8)	0.675(6)	0.531(−13)	0.646(−12)	0.405(−11)	0.868(−11)
18	0.494(−8)	0.629(−8)	0.679(6)	0.468(−14)	0.211(−14)	0.620(−13)	0.352(−14)
24	0.491(−8)	0.530(−8)	0.679(6)	0.567(−15)	0.324(−15)	0.103(−14)	0.337(−13)
34	0.493(−8)	0.520(−8)	0.676(6)	0*	0.162(−15)	0.124(−14)	0.317(−13)
36	0.494(−8)	0.520(−8)	0.679(6)	0.850(−15)	0.324(−15)	0.103(−14)	0.308(−13)

* The errors less than computer rounding errors in double precision.

and the highly accurate leading coefficients are natural consequences.

3. Error bounds and integration approximation

Define the norm

$$\|v\|_1 = \|v\|_{1,S} = \left[\int\int_S (v^2 + v_x^2 + v_y^2)\mathrm{d}s\right]^{1/2}.$$

We cite a lemma from Refs. [14,16].

Lemma 3.1. *Let $u \in H^1(S)$ be the solution of Motz's problem. If the following inverse property holds*

$$\|v_\nu\|_{0,\overline{AB}} \le K_N \|v\|_1, \qquad v \in V_N, \tag{3.1}$$

where

$$\|v_\nu\|_{0,\overline{AB}} = \left\{\int_{\overline{AB}} v_\nu^2 \,\mathrm{d}\ell\right\}^{1/2}.$$

Then for any $w > 0$, there exists a constant C independent of N and u such that

$$\|u - u_N\|_1 \le C\left(K_N + \frac{1}{w}\right)\|u - u_N\|_B.$$

Below, new analysis is devoted to the collocation Trefftz method involving numerical approximation of integration.

Table 4
The error norms and condition numbers from the collocation Trefftz method for Motz's problem by different Gaussian rules with r nodes as $N = 34$

r Nodes	M	$\|\varepsilon\|_B$	$\|\varepsilon\|_{\infty,\overline{AB}}$	Cond.	$\left\|\frac{\Delta D_0}{D_0}\right\|$	$\left\|\frac{\Delta D_1}{D_1}\right\|$	$\left\|\frac{\Delta D_2}{D_2}\right\|$	$\left\|\frac{\Delta D_3}{D_3}\right\|$
1	24	0.839(−8)	0.459(−8)	0.606(6)	0.169(−11)	0.121(−10)	0.296(−10)	0.152(−10)
2	24	0.854(−8)	0.369(−8)	0.672(6)	0.708(−13)	0.512(−12)	0.133(−11)	0.106(−11)
4	24	0.610(−8)	0.540(−8)	0.679(6)	0.425(−15)	0.535(−14)	0.641(−13)	0.755(−13)
6	30	0.493(−8)	0.520(−8)	0.676(6)	0*	0.162(−15)	0.124(−14)	0.317(−13)
8	24	0.428(−8)	0.519(−8)	0.679(6)	0.142(−15)	0.648(−15)	0.618(−15)	0.315(−13)
10	20	0.639(−8)	0.521(−8)	0.679(6)	0.142(−15)	0*	0.412(−15)	0.308(−13)

* The errors less than computer rounding errors in double precision.

Table 5
The leading coefficients D_i from the collocation Trefftz method for Motz's problem by the Gaussian rule with six nodes as $N=34$ and $M=30$

i	All digits	Significant digits	Number of significant digits
0	401.162453745234416	401.16245374523442	17
1	87.6559201950879299	87.6559201950879	15
2	17.2379150794467897	17.2379150794468	15
3	−8.0712152596987790	−8.07121525970	12
4	1.44027271702238968	1.44027271702	12
5	0.331054885920006037	0.33105488592	12
6	0.275437344507860671	0.27543734451	11
7	−0.869329945041107943(−1)	−0.869329945(−1)	9
8	0.336048784027428854(−1)	0.336048784(−1)	9
9	0.153843744594011413(−1)	0.153843745(−1)	9
10	0.730230164737157971(−2)	0.7302302(−2)	7
11	−0.318411361654662899(−2)	−0.3184114(−2)	7
12	0.122064586154974736(−2)	0.1220646(−2)	7
13	0.530965295822850803(−3)	0.530965(−3)	6
14	0.271512022889081647(−3)	0.271512(−3)	6
15	−0.120045043773287966(−3)	−0.12005(−3)	5
16	0.505389241414919585(−4)	0.5054(−4)	4
17	0.231662561135488172(−4)	0.2317(−4)	4
18	0.115348467265589439(−4)	0.11535(−4)	5
19	−0.529323807785491411(−5)	−0.529(−5)	3
20	0.228975882995988624(−5)	0.229(−5)	3
21	0.106239406374917051(−5)	0.106(−5)	3
22	0.530725263258556923(−6)	0.531(−6)	3
23	−0.245074785537844696(−6)	−0.25(−6)	2
24	0.108644983229739802(−6)	0.11(−6)	2
25	0.510347415146524412(−7)	0.5(−7)	1
26	0.254050384217598898(−7)	0.3(−7)	1
27	−0.110464929421918792(−7)	−0.1(−7)	1
28	0.493426255784041972(−8)	/	0
29	0.232829745036186828(−8)	/	0
30	0.115208023942516515(−8)	/	0
31	−0.345561696019388690(−9)	/	0
32	0.153086899837533823(−9)	/	0
33	0.722770554189099639(−10)	/	0
34	0.352933005315648864(−10)	/	0

Denote

$$[u,v]_{\tilde{B}} = \left\{ \tilde{\int}_{\overline{AB}} uv\,\mathrm{d}\ell + w^2 \tilde{\int}_{\overline{BC}\cup\overline{CD}} u_\nu v_\nu\,\mathrm{d}\ell \right\}^{1/2}, \qquad (3.2)$$

$$\|v\|_{\tilde{B}} = \sqrt{[v,v]_{\tilde{B}}} = \left\{ \tilde{\int}_{\overline{AB}} v^2\,\mathrm{d}\ell + w^2 \tilde{\int}_{\overline{BC}\cup\overline{CD}} v_\nu^2\,\mathrm{d}\ell \right\}^{1/2}. \qquad (3.3)$$

The solutions $\tilde{u}_N$ of Eq. (2.15) will satisfy

$$\|u-\tilde{u}_N\|_{\tilde{B}} = \min_{v\in V_N} \|u-v\|_{\tilde{B}} = \min_{v\in V_N} \sqrt{\tilde{I}(v)}. \qquad (3.4)$$

For the integration rules involved, we denote

$$\|v\|_{\tilde{B}}^2 = \|\hat{v}\|_B^2, \qquad (3.5)$$

where $\tilde{v}^2$ are piecewise interpolation polynomials of v^2 with order k along $\Gamma = \partial S$. We can prove the following lemma, similarly from Refs. [14,16].

Lemma 3.2. *The solutions $\tilde{u}_N$ obtained by the collocation Trefftz methods with integral approximation satisfy*

$$[u-\tilde{u}_N, v]_{\tilde{B}} = 0, \qquad \forall v \in V_N, \qquad (3.6)$$

and

$$\|v-\tilde{u}_N\|_{\tilde{B}} \le \|u-v\|_{\tilde{B}}, \qquad \forall v \in V_N. \qquad (3.7)$$

Table 6
The errors and condition numbers from the collocation Trefftz method by the central rule for the cracked beam problem with u_N, where $w = 1/(N+1)$

$N+1$	$\|u-u_N\|_B$	$\|u-u_N\|_{\infty,\overline{BC}}$	Cond.
12	0.174(−1)	0.192(−1)	118
20	0.103(−3)	0.143(−3)	0.242(4)
28	0.780(−6)	0.126(−5)	0.457(5)
36	0.697(−8)	0.123(−7)	0.828(6)
44	0.655(−10)	0.128(−)	0.148(8)

Table 7
The coefficients from the collocation Trefftz method by the central rule for the cracked beam problem with u_N as $N=43$

i	$\hat{D}_i$	i	$\hat{D}_i$
0	540.565122713627	22	0.741136835680306(−12)
1	−167.041350909274	23	0.417873188876248(−11)
2	0.198198742457744(−13)	24	−0.121996855522588(−7)
3	−0.219185365289299(−13)	25	−0.143269204396301(−6)
4	−2.21801471698044	26	0.853944744811233(−12)
5	−1.68233110389621	27	0.392784692715081(−11)
6	−0.214659464703740(−14)	28	−0.519522874909708(−9)
7	0.975152635890286(−14)	29	−0.716697851376144(−8)
8	−0.722712676630922(−2)	30	0.562441620804752(−12)
9	−0.419620077504757(−1)	31	0.210052519224617(−11)
10	0.158368581564262(−13)	32	−0.226112209663434(−10)
11	0.977095083882188(−13)	33	−0.361688092767140(−9)
12	−0.349003797729518(−3)	34	0.209940550959741(−12)
13	−0.154580008052455(−2)	35	0.631754175553925(−12)
14	0.893242771123692(−13)	36	−0.907100573484872(−12)
15	0.733457764014275(−12)	37	−0.166314437291397(−10)
16	−0.824172461669611(−5)	38	0.411725887639002(−13)
17	−0.649512698211018(−4)	39	0.988154926645705(−13)
18	0.356068309179608(−12)	40	−0.230535024761913(−13)
19	0.244904048630545(−11)	41	−0.493264784148099(−12)
20	−0.317915391408544(−6)	42	0.328644957534978(−14)
21	−0.296970610620140(−5)	43	0.621165127407370(−14)

Next, let us examine the errors from integration rules. Suppose that the rules are chosen to have the following relative errors for v and $u-v$, where $v \in V_N$

$$\frac{\left|\left(\int_{\overline{AB}} - \tilde{\int}_{\overline{AB}}\right) v^2 \,\mathrm{d}\ell\right|}{\int_{\overline{AB}} v^2 \,\mathrm{d}\ell} \le b < \frac{3}{4}, \tag{3.8}$$

$$\frac{\left|\left(\int_{\overline{BC}} - \tilde{\int}_{\overline{BC}}\right) v_\nu^2 \,\mathrm{d}\ell\right|}{\int_{\overline{BC}} v_\nu^2 \,\mathrm{d}\ell} \le b < \frac{3}{4}, \tag{3.9}$$

$$\frac{\left|\left(\int_{\overline{CD}} - \tilde{\int}_{\overline{CD}}\right) v_\nu^2 \,\mathrm{d}\ell\right|}{\int_{\overline{CD}} v_\nu^2 \,\mathrm{d}\ell} \le b < \frac{3}{4}, \tag{3.10}$$

Table 8
The errors and condition numbers from the collocation Trefftz method by the central rule for the cracked beam problem with u_N^*, where $w = 1/(N+1)$

$N+1$	$\Vert u-u_N^*\Vert_B$	$\Vert u-u_N^*\Vert_{\infty,\overline{BC}}$	Cond.
12	0.181(−1)	0.143(−1)	14.7
20	0.108(−3)	0.860(−4)	179
28	0.835(−6)	0.673(−6)	0.241(4)
36	0.731(−8)	0.593(−8)	0.340(5)
44	0.689(−10)	0.563(−10)	0.492(6)

Table 9
The coefficients from the collocation Trefftz method by the central rule for the cracked beam problem with u_N^* as $N=43$

i	$\hat{D}_i$	i	$\hat{D}_i$
0	540.565122713627	21	−0.296970704226108(−5)
1	−167.041350909274	24	−0.122002935723549(−7)
4	−2.21801471698038	25	−0.143270030434461(−6)
5	−1.68233110389617	28	−0.519982420026741(−9)
8	−0.722712676632975(−2)	29	−0.716735060983968(−8)
9	−0.419620077505017(−1)	32	−0.228004937465962(−10)
12	−0.349003797758166(−3)	33	−0.361766490834198(−9)
13	−0.154580008066482(−2)	36	−.0946724588701563(−12)
16	−0.824172478281220(−5)	37	−0.166363445310374(−10)
17	−0.649512703568597(−4)	40	−0.263335130630466(−13)
20	−0.317915829660462(−6)	41	−0.492957376797978(−12)

where b is a constant. Then we have the following proposition.

Proposition 3.1. *For those rules of quadrature satisfying Eqs.* (3.8)–(3.10), *the following bound holds*

$$\left|\frac{\Vert v\Vert_B - \Vert v\Vert_{\tilde{B}}}{\Vert v\Vert_B}\right| \le a < \frac{1}{2}, \qquad v \in V_N, \tag{3.11}$$

where $a = 1-\sqrt{1-b}$ *is a constant.*

Proof. We have from the assumptions

$$\frac{|\Vert v\Vert_B^2 - \Vert v\Vert_{\tilde{B}}^2|}{\Vert v\Vert_B^2} \le \frac{\left|\left(\int_{\overline{AB}} - \tilde{\int}_{\overline{AB}}\right) v^2 \,\mathrm{d}\ell + \left(\int_{\overline{BC}\cup\overline{CD}} - \tilde{\int}_{\overline{BC}\cup\overline{CD}}\right) v_\nu^2 \,\mathrm{d}\ell\right|}{\int_{\overline{AB}} v^2 \,\mathrm{d}\ell + \int_{\overline{BC}\cup\overline{CD}} v_\nu^2 \,\mathrm{d}\ell} \le b. \tag{3.12}$$

We obtain

$$1-b \le \frac{\Vert v\Vert_{\tilde{B}}^2}{\Vert v\Vert_B^2} \le 1+b.$$

The above equation gives

$$\sqrt{1-b} \le \frac{\Vert v\Vert_{\tilde{B}}}{\Vert v\Vert_B} \le \sqrt{1+b}. \tag{3.13}$$

Next, we have from Eqs. (3.12) and (3.13)

$$\frac{|\Vert v\Vert_B - \Vert v\Vert_{\tilde{B}}|}{\Vert v\Vert_B} \le \frac{b}{\Vert v\Vert_B + \Vert v\Vert_{\tilde{B}}}\Vert v\Vert_B \le \frac{b}{1+\frac{\Vert v\Vert_{\tilde{B}}}{\Vert v\Vert_B}}$$

$$\le \frac{b}{1+\sqrt{1-b}} = 1-\sqrt{1-b} = a < \frac{1}{2}. \tag{3.14}$$

This completes the proof of Proposition 3.1. □

Table 10
The error norms and condition numbers from the collocation Trefftz method for the cracked beam problem as $N=43$ by the Gaussian rule with eight nodes

M	$\|u-u_N^*\|_B$	$\|u-u_N^*\|_{\infty,\overline{BC}}$	Cond.	$\left\|\frac{\Delta\hat{D}_0}{\hat{D}_0}\right\|$	$\left\|\frac{\Delta\hat{D}_1}{\hat{D}_1}\right\|$	$\left\|\frac{\Delta\hat{D}_4}{\hat{D}_4}\right\|$	$\left\|\frac{\Delta\hat{D}_5}{\hat{D}_5}\right\|$
16	0.317(−10)	0.579(−10)	0.447(6)	0.421(−15)	0.340(−15)	0.340(−14)	0.647(−14)
24	0.319(−10)	0.527(−10)	0.447(6)	0*	0.510(−15)	0.701(−14)	0.103(−13)
32	0.319(−10)	0.526(−10)	0.447(6)	0.841(−15)	0.340(−15)	0.541(−14)	0.594(−14)
40	0.319(−10)	0.526(−10)	0.447(6)	0.631(−15)	0*	0.801(−15)	0.792(−14)

* The errors less than computer rounding errors in double precision.

Take the central rule in Eqs. (2.12) and (2.13) for example. We have from Ref. [1]

$$\left(\int_{\overline{AB}}-\tilde{\int}_{\overline{AB}}\right)f\,\mathrm{d}\ell=\frac{h^2}{24}f''(\xi), \tag{3.15}$$

where $f=v^2$ or $f=(u-v)^2$, and $\xi\in\overline{AB}$. Since $f''=2\{(v')^2+vv''\}$ for $f=v^2$, the requirements of quadrature errors in Proposition 3.1 imply that

$$\frac{1}{4}\int_{\overline{AB}}v^2\,\mathrm{d}\ell\le\tilde{\int}_{\overline{AB}}v^2\,\mathrm{d}\ell\le\frac{7}{4}\int_{\overline{AB}}v^2\,\mathrm{d}\ell, \tag{3.16}$$

or equivalently

$$\frac{h^2}{12}|((v')^2+vv'')(\xi)|\le\frac{3}{4}\int_{\overline{AB}}v^2\,\mathrm{d}\ell. \tag{3.17}$$

Next, we give a new lemma.

Lemma 3.3. *Suppose that the rules of integrations in Eq.* (2.16) *are chosen to satisfy the bound* (3.11). *Then, the norms* $\|\cdot\|_B$ *and* $\|\cdot\|_{\tilde{B}}$ *defined in Eqs.* (2.11) and (3.3) *are equivalent to each other*

$$C_1\|v\|_B\le\|v\|_{\tilde{B}}\le C_2\|v\|_B,\qquad v\in V_N, \tag{3.18}$$

where C_1 *and* C_2 *are two positive constants independent of* v *and* N.

Proof. We have from Eq. (3.11)

$$\|v\|_B-\|v\|_{\tilde{B}}\le a\|v\|_B,$$

and then

$$\|v\|_B\le\frac{1}{1-a}\|v\|_{\tilde{B}}. \tag{3.19}$$

Also from Eq. (3.11)

$$\|v\|_{\tilde{B}}-\|v\|_B\le a\|v\|_B,$$

and then

$$\|v\|_{\tilde{B}}\le(1+a)\|v\|_B. \tag{3.20}$$

Hence, the desired result (3.18) follows from Eqs. (3.19) and (3.20). This completes the proof of Lemma 3.3. □

Accordingly, we have a new, important theorem.

Theorem 3.1. *Let the condition* (3.1) *hold, and the rules of integrations involved in Eq.* (2.16) *satisfy Eq.* (3.11) *for* v *and* $u-v$, $\forall v\in V_N$. *Then*

$$\|u-\tilde{u}_N\|_1\le\inf_{v\in V_N}\{\|u-v\|_1+C(K_N+1/w)\|u-v\|_B\}, \tag{3.21}$$

where C is a bounded constant independent of u, v and N. *Moreover*

$$\|u-\tilde{u}_N\|_1\le\|R_N\|_1+C(K_N+1/w)\|R_N\|_B, \tag{3.22}$$

where

$$R_N=\sum_{i=N+1}^{\infty}d_ir^{i+(1/2)}\cos\left(i+\frac{1}{2}\right)\theta, \tag{3.23}$$

and d_i *are the true expansion coefficients.*

Table 11
The error norms and condition numbers from the collocation Trefftz method for the cracked beam problem by different Gaussian rules with r nodes as $N=43$

r	M	$\|u-u_N^*\|_B$	$\|u-u_N^*\|_{\infty,\overline{BC}}$	Cond.	$\left\|\frac{\Delta\hat{D}_0}{\hat{D}_0}\right\|$	$\left\|\frac{\Delta\hat{D}_1}{\hat{D}_1}\right\|$	$\left\|\frac{\Delta\hat{D}_4}{\hat{D}_4}\right\|$	$\left\|\frac{\Delta\hat{D}_5}{\hat{D}_5}\right\|$
1	24	0.614(−10)	0.102(−9)	0.434(6)	0.294(−14)	0.715(−14)	0.177(−12)	0.175(−12)
2	24	0.623(−10)	0.602(−0)	0.446(6)	0.210(−15)	0.187(−14)	0.617(−13)	0.523(−13)
4	24	0.448(−10)	0.519(−10)	0.446(6)	0.210(−15)	0.119(−14)	0.921(−14)	0.462(−14)
6	24	0.367(−10)	0.576(−10)	0.447(6)	0.210(−15)	0*	0.661(−14)	0.726(−14)
8	24	0.319(−10)	0.527(−10)	0.447(6)	0*	0.510(−15)	0.701(−14)	0.103(−13)
12	24	0.261(−10)	0.524(−10)	0.447(6)	0.210(−15)	0.340(−15)	0.741(−14)	0.488(−14)

* The errors less than computer rounding errors in double precision.

Table 12
The leading coefficients from the collocation Trefftz method for the cracked beam problem by the Gaussian rule with eight nodes as $N = 43$ and $M = 24$.

i	$\hat{D}_i$
0	540.565122713627488338
1	−167.041350909274314063
4	−2.21801471698042096392
5	−1.68233110389623896630
8	−0.722712676629304936332(−2)
9	−0.419620077504989710815(−1)
12	−0.349003797752273547863(−3)
13	−0.154580008073283248042(−2)
16	−0.824172472675852766202(−5)
17	−0.649512707503007010942(−4)
20	−0.317915648270962735950(−6)
21	−0.296970804065775927138(−5)
24	−0.122000024043979050718(−7)
25	−0.143271318148128170607(−6)
28	−0.519737845303284863567(−9)
29	−0.716825117065194526952(−8)
32	−0.226916180319381751640(−10)
33	−0.362109309069568822496(−9)
36	−0.922553631817261539388(−12)
37	−0.167027744142682193722(−10)
40	−0.242365241977693826580(−13)
41	−0.498065701032834816745(−12)

Proof. From Refs. [14,16], we have

$$\|v\|_1 \le C(K_N + 1/w)\|v\|_B, \qquad \forall v \in V_N. \tag{3.24}$$

The constant C in this paper is used as a generic, bounded constant; their values may be different in different contexts. Let $\eta = v - \tilde{u}_N$, then $\eta \in V_N$ if $v \in V_N$. In view of Eq. (3.24) and the norm equivalence (3.18)

$$\|u - \tilde{u}_N\|_1 \le \|u - v\|_1 + \|\eta\|_1$$
$$\le \|u - v\|_1 + C(K_N + 1/w)\|\eta\|_B$$
$$\le \|u - v\|_1 + \frac{C}{C_1}(K_N + 1/w)\|\eta\|_{\tilde{B}}. \tag{3.25}$$

From the orthogonal property (3.6) we obtain

$$\|\eta\|_{\tilde{B}}^2 = [\eta, \eta]_{\tilde{B}} = [v - u, \eta]_{\tilde{B}} \le \|u - v\|_{\tilde{B}}\|\eta\|_{\tilde{B}}. \tag{3.26}$$

The above bound and the norm equivalence for $u - v$ leads to

$$\|\eta\|_{\tilde{B}} \le \|u - v\|_{\tilde{B}} \le C\|u - v\|_B. \tag{3.27}$$

Combining Eqs. (3.25) and (3.27) gives the first desired result (3.21).

Next, the solution (1.4) with the true coefficients d_i can be split into

$$u = \tilde{u}_N + R_N, \tag{3.28}$$

where

$$\bar{u}_N = \sum_{i=0}^{N} d_i r^{i+(1/2)} \cos\left(i + \frac{1}{2}\right)\theta, \tag{3.29}$$

and the remainder R_N is given by Eq. (3.23). Then let $v = \bar{u}_N$ in Eq. (3.21) we obtain

$$\|u - \tilde{u}_N\|_1 \le \|u - \bar{u}_N\|_1 + C(K_N + 1/w)\|u - \bar{u}_N\|_B$$
$$\le \|R_N\|_1 + C(K_N + 1/w)\|R_N\|_B. \tag{3.30}$$

Table 13
The leading coefficients α_i from Table 12 by Eq. (5.5) for $a = 1/2$ and $b = .0125$ in the scaled cracked beam problem

i	All digits	Significant digits	Number of significant digits
0	0.191118631971872093844	0.19111863197187209	17
1	−0.118116071966509542102	−0.1181160719665095	16
4	−0.125469859771873346044(−1)	−0.12546985977187(−1)	14
5	−0.190334037082572939126(−1)	−0.19033403708257(−1)	14
8	−0.654124844152399417298(−3)	−0.65412484415(−3)	11
9	−0.759593477954055400214(−2)	−0.759593477954(−2)	12
12	−0.505411485799405575323(−3)	−0.5054114858(−3)	10
13	−0.447711526684630486267(−2)	−0.447711527(−2)	9
16	−0.190964676787037826271(−3)	−0.19096468(−3)	8
17	−0.300990359104527302470(−2)	−0.3009904(−2)	7
20	−0.117860105316055165819(−3)	−0.117860(−3)	6
21	−0.220190546979016346305(−2)	−0.220191(−2)	6
24	−0.723660418005184549999(−4)	−0.7237(−4)	4
25	−0.169966822206286320533(−2)	−0.1700(−2)	4
28	−0.493263780013297154056(−4)	−0.49(−4)	2
29	−0.136062389932649135602(−2)	−0.136(−2)	3
32	−0.344572276541308970127(−4)	−0.3(−4)	1
33	−0.109972615269026243248(−2)	−0.1(−2)	1
36	−0.224143667286699527393(−4)	/	0
37	−0.811621347953916006009(−3)	/	0
40	−0.942161102160732748267(−5)	/	0
41	−0.387232200462756144532(−3)	/	0

Table 14
The error norms and condition numbers from the collocation Trefftz method directly for the traditional cracked beam problem in Fig. 3Fig. 3. The traditional cracked beam problem in $\hat{S}$. by different Gaussian rules with different nodes as $N = 43$.

r	M	$\|w - w_N^*\|_B$	$\|w - w_N^*\|_{\infty,\overline{BC}}$	Cond.	$\left\|\frac{\Delta\hat{D}_0}{\hat{D}_0}\right\|$	$\left\|\frac{\Delta\hat{D}_1}{\hat{D}_1}\right\|$	$\left\|\frac{\Delta\hat{D}_4}{\hat{D}_4}\right\|$	$\left\|\frac{\Delta\hat{D}_5}{\hat{D}_5}\right\|$
1	24	0.180(−13)	0.159(−13)	0.191(10)	0.203(−14)	0.493(−14)	0.142(−12)	0.140(−12)
2	24	0.160(−13)	0.141(−13)	0.191(10)	0*	0.141(−14)	0.684(−13)	0.483(−13)
4	24	0.116(−13)	0.141(−13)	0.187(10)	0.102(−14)	0.940(−15)	0.124(−13)	0.140(−13)
6	24	0.955(−14)	0.144(−13)	0.186(10)	0*	0.117(−15)	0.111(−14)	0.729(−15)
8	24	0.833(−14)	0.143(−13)	0.185(10)	0.290(−15)	0.235(−15)	0.166(−14)	0.365(−14)
12	24	0.680(−14)	0.143(−13)	0.185(10)	0.145(−15)	0.117(−15)	0.138(−15)	0.419(−14)

* The errors less than computer rounding errors in double precision.

This is the second bound (3.22) as desired, which completes the proof of Theorem 3.1. □

Even for the simplest central rule, the relative errors of its approximate integrals has no difficult to be less than three quarters. So the conditions (3.8)–(3.11) can be satisfied easily. Hence, the solutions $\tilde{u}_N$ may still have the exponential convergence rates. More explanation will be given in Section 5. This is a significant difference from the traditional role of integration in the finite element analysis. Besides, from Theorem 3.1, there is not much difference between lower-order and higher-order quadratures. However, for the accuracy of the leading coefficient D_0, the high-order rules, such as the Gaussian quadratures with six and eight nodes, may raise its accuracy, based on Tables 3 and 4. Note that the new analysis of quadratures in this section provides a theoretical foundation for the high accuracy of the collocation Trefftz method.

4. The cracked beam problem

As a variant of Motz's problem, the cracked beam problem is discussed here. Its highly accurate solution can be sought similarly by the collocation Trefftz method (e.g. the BAM in Refs. [14,16]). Not only its highly accurate solutions are obtained in this paper, but also the highly accurate leading coefficient in double precision can be achieved by the Gaussian rule. Half of its expansion coefficients are zero, which is supported by a posterior analysis. Hence, as a singularity model, the cracked beam problem given in this section seems to be superior to Motz's problem in Sections 2 and 3.

Table 15
The leading coefficients α_i from the collocation Trefftz method directly from the traditional cracked beam problem in Fig. 3 by the Gaussian rule with six nodes as $N = 43$ and $M = 24$

i	All digits	Significant digits	Number of significant digits
0	0.19111863197187209384 4	0.19111863197187209	17
1	−0.1181160719665095588 35	−0.1181160719665095	16
4	−0.125469859771874230753(−1)	−0.125469859771874(−1)	15
5	−0.190334037082570510513(−1)	−0.190334037082571(−1)	15
8	−0.654124844153439167181(−3)	−0.65412484415(−3)	11
9	−0.759593477953802304059(−2)	−0.759593477954(−2)	12
12	−0.505411485758066030688(−3)	−0.5054114858(−3)	10
13	−0.447711526664487571153(−2)	−0.447711527(−2)	9
16	−0.190964673066832069321(−3)	−0.1909647(−3)	7
17	−0.300990357223324123126(−2)	−0.3009904(−2)	7
20	−0.117859936451135464920(−3)	−0.11786(−3)	5
21	−0.220190469161906385645(−2)	−0.22019(−2)	5
24	−0.723620522995536540750(−4)	−0.724(−4)	3
25	−0.169965180428740376094(−2)	−0.1700(−2)	4
28	−0.492760129615704093459(−4)	−0.49(−4)	2
29	−0.136043628609274110108(−2)	−0.136(−2)	3
32	−0.341170517533278386583(−4)	−0.3(−4)	1
33	−0.109855994151387601453(−2)	−0.1(−2)	1
36	−0.212639663103781256836(−4)	/	0
37	−0.807933182726571115506(−3)	/	0
40	−0.789995944027442427633(−5)	/	0
41	−0.382605289154327110005(−3)	/	0

Table 16
Comparisons of the error norms and condition numbers from Table 11 by Eq. (5.9) and directly from the traditional cracked beam problem in Fig. 3 as $N = 43$ and $M = 24$

r Nodes	From Table 11 by Eq. (5.9)			Direct computation		
	$(b/500)\cdot\|u-u_N^*\|_B$	$(b/500)\cdot\|u-u_N^*\|_{\infty,\overline{BC}}$	Cond.	$\|w-w_N^*\|_B$	$\|w-w_N^*\|_{\infty,\overline{BC}}$	Cond.
1	0.154(−14)	0.255(−14)	0.434(6)	0.180(−13)	0.159(−13)	0.191(10)
2	0.156(−14)	0.151(−14)	0.446(6)	0.160(−13)	0.141(−13)	0.191(10)
4	0.112(−14)	0.130(−14)	0.446(6)	0.116(−13)	0.141(−13)	0.187(10)
6	0.918(−15)	0.144(−14)	0.447(6)	0.955(−14)	0.144(−13)	0.186(10)
8	0.798(−15)	0.132(−14)	0.447(6)	0.833(−14)	0.143(−13)	0.185(10)
12	0.653(−15)	0.131(−14)	0.447(6)	0.680(−14)	0.143(−13)	0.185(10)

When the boundary conditions on $\overline{AB}$ and on $\overline{BC}$ in Fig. 1 are exchanged as (Fig. 2)

$$u|_{\overline{BC}} = 500,\ \ u|_{\overline{OD}} = 0,\ \ u_\nu|_{\overline{OA}} = 0,\ \ u_\nu|_{\overline{AB}\cup\overline{CD}} = 0, \quad (4.1)$$

this Laplace boundary value problem gives the cracked beam problem. Its original model in Refs. [4–6,19,21] was defined on the domain

$$\hat{S} = \{(x,y)| -\tfrac{1}{2} \le x \le \tfrac{1}{2}, 0 \le y \le \tfrac{1}{2}\}$$

in Fig. 3. However, two models in S and $\hat{S}$ have the same nature. In fact, their solutions can be scaled from one to the other, which will be explained in Section 5. Since function (1.4) is also the solutions of the cracked beam problem, we choose

$$u_N(r,\theta) = \sum_{i=0}^{N} \hat{D}_i r^{i+(1/2)} \cos\left(i+\frac{1}{2}\right)\theta, \quad (4.2)$$

where the notations $\hat{D}_i$ with a hat on its head are used to distinguish with those D_i of Motz's problem in Section 2. We also use V_N as the finite collection of function (4.2). Since u_N satisfies the Laplace equation in S and the boundary conditions on $\overline{OD}\cup\overline{OA}$ already, the coefficients $\hat{D}_i$ should be chosen to satisfy the rest boundary conditions as best as possible. Define the error norm on $\overline{AB}\cup\overline{BC}\cup\overline{CD}$:

$$\|u-v\|_B = \left\{\int_{\overline{BC}} (v-500)^2 + w^2 \int_{\overline{AB}\cup\overline{CD}} v_\nu^2\right\}^{1/2}, \quad w = \frac{1}{N+1}. \quad (4.3)$$

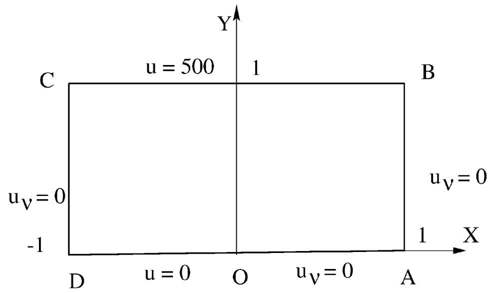

Fig. 2. The cracked beam problem.

The solution u_N can be obtained by

$$\|u-u_N\|_{\tilde{B}} = \inf_{v\in V_N} \|u-v\|_{\tilde{B}}, \quad (4.4)$$

where

$$\|v\|_{\tilde{B}} = \left\{\tilde{\int}_{\overline{BC}} v^2 + w^2 \tilde{\int}_{\overline{AB}\cup\overline{CD}} v_\nu^2\right\}^{1/2}. \quad (4.5)$$

We first employ the central rule with a uniform distributed points P_i on $\overline{AB}\cup\overline{BC}\cup\overline{CD}$. We may require $\sqrt{h}v = \sqrt{h}500$ at $P_i \in \overline{BC}$ and $\sqrt{h}wu_\nu = 0$ at $P_i \in \overline{AB}\cup\overline{CD}$. Let the number $4M$ of all collocation nodes P_i be larger than $N+1$, then we obtain an overdetermined system of linear algebraic equations $\mathbf{F}\vec{x} = \vec{b}$, where $\mathbf{F}$ is a matrix of $4M\times(N+1)$, and $\vec{x}$ is the unknown vector consisting of $\vec{D}_i$. We employ the LSM in Section 2 to solve it. The errors, condition numbers and the leading coefficients are given in Tables 6 and 7. It is interesting from Table 7 to note that $\hat{D}_{4\ell+2} \approx \hat{D}_{4\ell+3} \approx 0$.[3] Hence, we may simply seek a solution of the following simplified forms

$$u_N^* = \sum_{\ell=0}^{L}\sum_{k=0}^{1} \hat{D}_{4\ell+k} r^{4\ell+k+(1/2)} \cos\left(4\ell+k+\frac{1}{2}\right)\theta, \quad (4.6)$$

where $N = 4L+1$. Denote by V_N^* the finite collection of functions in Eq. (4.6). Hence another collocation Trefftz method can be formulated as in Section 2: to seek the solution $u_N^* \in V_N^*$ such that

$$\|u-u_N^*\|_{\tilde{B}} = \inf_{v\in V_N^*} \|u-v\|_{\tilde{B}}, \quad (4.7)$$

where $\|v\|_{\tilde{B}}$ is defined in Eq. (4.5). Its results are given in Tables 8 and 9. From Tables 6 and 8, we have observed the asymptotes:

$$\|u-u_N\|_B = O(0.553^N),\ \ \|u-u_N\|_{\infty,\overline{BC}} = O(0.564^N),\ \ \text{Cond.} = O(1.42^N), \quad (4.8)$$

[3] This fact has been double checked under Mathmatica system using high working digits and more expansion terms. In fact, u_{400} has been obtained in Ref. [22], which clearly shows that $\hat{D}_{4\ell+2} \approx \hat{D}_{4\ell+3} \approx 0$.

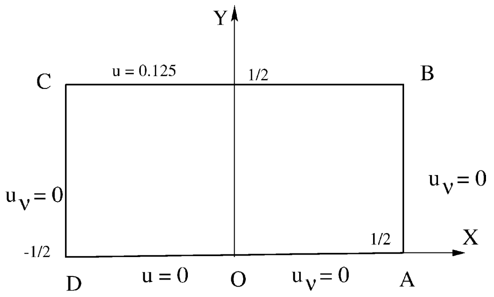

Fig. 3. The traditional cracked beam problem in $\hat{S}$.

$$\|u - u_N^*\|_B = O(0.558^N), \quad \|u - u_N^*\|_{\infty,\overline{BC}} = O(0.558^N),$$
$$\text{Cond.} = O(1.39^N). \tag{4.9}$$

Note that the convergence rates and the condition numbers in Eq. (4.9) are close to those in Eq. (4.8), but only half coefficients of u_N in Eq. (4.2) are needed. Hence, for the computational purpose, the solution (4.6) with Tables 8 and 9 may better be chosen. From this point of view, the cracked beam using Eq. (4.6) may serve as a better testing model of singularity problems than Motz's problem.

Compared with the more accurate solutions from CTM [22] using Mathematica with more working digits, the leading coefficients $\hat{D}_0$ and $\hat{D}_1$ in Table 9 have 15 significant digits.

The analysis in Section 3 can be similarly applied to the collocation Trefftz method for the cracked beam problem. To confirm the admissible functions as Eq. (4.6), we only prove the following proposition.

Proposition 4.1. *Let the errors* $\varepsilon_N = u - u_N^*$, $N = 4L + 1$ *and*

$$\|(\varepsilon_N)_\nu\|_{0,\overline{BC}} \le K_N \|\varepsilon_N\|_{1,S}, \tag{4.10}$$

where the constant $K_N (\ge 1)$ *may be unbounded as* $N \to \infty$. *Suppose*

$$\left(K_N + \frac{1}{w}\right)\|\varepsilon_N\|_B \to 0, \qquad \text{as } N \to \infty. \tag{4.11}$$

Then the solution of the cracked beam problem can be expressed by

$$u = \sum_{\ell=0}^{\infty} \sum_{k=0}^{1} \hat{D}_{4\ell+k} r^{4\ell+k+(1/2)} \cos\left(4\ell + k + \frac{1}{2}\right)\theta. \tag{4.12}$$

Proof. From the bounds similar to Lemma 3.1, we have

$$\|\varepsilon_N\|_{1,S} = \|u - u_N^*\|_{1,S} \le C\left(K_N + \frac{1}{w}\right)\|\varepsilon_N\|_B, \tag{4.13}$$

where C is a bounded constant independent of N. From Eqs. (4.11) and (4.13), $\{\varepsilon_N\}$ is a bounded sequence. Based on the Kandrasov or Rellich theorem [2], any bounded sequence in the space $H^1(S)$ contains a subsequence that converges in $H^0(S)$. Then there must exist a subsequence $\{\varepsilon_N^+\}$ in $H^0(S)$ such that $\lim_{N\to\infty} \varepsilon_N^+ = \bar{\varepsilon}$. Since $\{\varepsilon_N^+\}$ are bounded in $H^1(S)$, the convergent limit $\bar{\varepsilon} \in H^1(S)$. This implies that

$$\lim_{N\to\infty} u_N^+ = \lim_{N\to\infty} (u - \varepsilon_N) = u - \bar{\varepsilon} = \bar{u} \in H^1(S).$$

Moreover, since $K_N \ge 1$ and $w = 1/(N+1)$, we conclude that $\|\bar{u} - 500\|_{0,\overline{BC}} = 0$ and $\|\bar{u}_\nu\|_{0,\overline{AB}\cup\overline{CD}} = 0$. Hence, $\bar{u}$ must be the unique solution of the cracked beam problem. Obviously, the entire sequence u_N^* also converges to $\bar{u}(=u)$ based on $\|u - u_N^*\|_B \to 0$ as $N \to \infty$ from Eqs. (4.11) and (4.13). This competes the proof of Proposition 4.1. □

When $w = 1/(N+1)$, the empirical exponential convergent rates in Eq. (4.9) guarantee Eq. (4.11). The analysis of Proposition 4.1 is made, based on the a posteriori numerical results, so we call it a posteriori analysis. Proposition 4.1 implies that $\tilde{D}_{4\ell+2} = \tilde{D}_{4\ell+3} = 0$, $\forall \ell \ge 0$. We also note that condition (4.11) is stronger than that $\|\varepsilon_N\|_B \to 0$ as $N \to \infty$.

Next, we pursue better accuracy of the leading coefficient $\hat{D}_0$ by using the Gaussian rules. Denote by M the collocation number along $\overline{AB}$, and then $4M$ is the total number of collocation nodes. First, we choose the Gaussian rule of eight nodes, and set the positions of collocation nodes as required, then its solutions and condition numbers by the collocation Trefftz method are listed in Table 10. Moreover, for the Gaussian rules with 1, 2, 4, 6, 8 and 12 nodes, their solution errors and condition numbers are listed in Table 11. The errors $\|u - u_N^*\|_B$ decrease nearly a half, from 0.614(−10) with $r = 1$ down to 0.319(−10) with $r = 8$. For $N = 43$ and $M = 24$, the leading coefficients $\tilde{D}_{4\ell+k}$, $k = 0, 1$ obtained by the Gaussian rule of eight nodes are reported in Table 12. Compared with the more accurate results in Ref. [22], the relative errors of

$$\hat{D}_0 = 540.565122713627488338,$$

from Table 12 has 17 significant digits, and $\hat{D}_1$ has 16 significant digits.

5. Discussions and comparisons

Let us consider the cracked beam problem on a scaled domain, $\hat{S} = \{(\xi, \eta) | -a < \xi < a, 0 < \eta < a\}$, where the parameter satisfies $0 < a \le 1$. The scaled cracked beam problem is described by the Laplace equation $\Delta w = 0$ on $\hat{S}$ satisfying the following boundary conditions

$$w(\xi, a) = b, \qquad -a < \xi < a, \tag{5.1}$$

$$w(\xi, 0) = 0, \qquad -a < \xi < 0, \quad \frac{\partial w}{\partial \nu}(\xi, 0) = 0, \quad 0 < \xi < a, \tag{5.2}$$

$$\frac{\partial w}{\partial \nu}(\pm a, \eta) = 0, \qquad 0 < \eta < a, \tag{5.3}$$

where b is a constant, and ν is the outward normal to $\partial \hat{S}$. Here, another Cartesian coordinate system (ξ, η) is chosen. For Fig. 2, $a = 1$ and $b = 500$, and for Fig. 3 from the traditional model [4–6,19,21], $a = 1/2$ and $b = 0.125$. The Laplace solution satisfying Eqs. (5.1)–(5.3) can also be expressed by

$$w(\xi, \eta) = \sum_{i=0}^{\infty} \alpha_i \rho^{i+(1/2)} \cos\left(i + \frac{1}{2}\right)\theta, \tag{5.4}$$

where α_i are the coefficients, (ρ, θ) are the polar coordinates at the origin o, and $\rho = \sqrt{\xi^2 + \eta^2}$. There exist the relations for the coefficients of $\hat{D}_i$ in Table 12 and α_i :

$$\alpha_i = \frac{b}{500} a^{-(i+(1/2))} \hat{D}_i. \tag{5.5}$$

Now, let us prove Eq. (5.5). Under the affine transformation $T : (x, y) \to (\xi, \eta)$, where $\xi = ax$ and $\eta = ay$, domain S is converted to $\hat{S}$, and the boundary conditions (4.1) are transformed to

$$u(\xi, a) = b, \qquad -a < \xi < a, \tag{5.6}$$

$$u(\xi, 0) = 0, \qquad -a < \xi < 0, \quad \frac{\partial u}{\partial \nu}(\xi, 0) = 0, \quad 0 < \xi < a, \tag{5.7}$$

$$\frac{\partial u}{\partial \nu}(\pm a, \eta) = 0, \qquad 0 < \eta < a. \tag{5.8}$$

Comparing Eq. (5.6) with $u|_{\overline{BC}} = 500$ in Eq. (4.1), we find the relations between w and u,

$$w = \frac{b}{500} u. \tag{5.9}$$

This gives

$$\sum_{i=0}^{\infty} \alpha_i \rho^{i+(1/2)} \cos\left(i + \frac{1}{2}\right)\theta = \frac{b}{500} \sum_{i=0}^{\infty} \hat{D}_i r^{i+(1/2)} \cos\left(i + \frac{1}{2}\right)\theta. \tag{5.10}$$

Since $r = \sqrt{x^2 + y^2}$, we have $r = \rho/a$. Eq. (5.10) is reduced to

$$\sum_{i=0}^{\infty} \left\{\alpha_i - \frac{b}{500} a^{-(i+(1/2))} \hat{D}_i\right\} \rho^{i+(1/2)} \cos\left(i + \frac{1}{2}\right)\theta = 0. \tag{5.11}$$

Since functions $\{\rho^{i+(1/2)} \cos(i + (1/2))\theta\}$ are linearly independent, we obtain

$$\alpha_i - \frac{b}{500} a^{-(i+(1/2))} \hat{D}_i = 0, \tag{5.12}$$

which is the desired equation (5.5).

By means of Eq. (5.5), the coefficients α_i can be obtained for $a = 1/2$ and $b = 0.125$, which are listed in Table 13. Our leading coefficients

$$\alpha_0 = 0.19111863197187209, \quad \alpha_1 = -0.1181160719665095, \tag{5.13}$$

from Table 13 have 17 and 16 significant digits, respectively, compared with the more accurate values:

$$\alpha_0 = 0.19111863197187208906830, \quad \alpha_1 = -0.11811607196650946846348. \tag{5.14}$$

Eq. (5.14) possessing 23 significant digits are cited from Ref. [22] by the same collocation Trefftz method but using higher working digits under Mathematica. Besides, the significant digits of other coefficients are also provided in Table 13, compared with more accurate α_i in Ref. [22].

We have also completed the direct computation for the traditional cracked beam problem in Fig. 3. The errors, condition numbers and the leading coefficients are listed in Tables 14–16. Interestingly, in Table 15, the same α_0 and α_1 as Eq. (5.13) are obtained. Let us compare two approaches: (1) from Table 12 by Eq. (5.5), (2) direct computation from Fig. 3. The global errors from Table 11 are 10 times smaller than those from direct computation (Table 16). On the other hand, the leading coefficients α_4 and α_5 from direct computation are slightly better than those in Table 13. We note that the condition number from the direct computation is huge, and the ratio of condition numbers between these two approaches is

$$\frac{\text{Cond.}|_{\text{Direct}}}{\text{Cond.}|_{\text{From Table 11}}} = \frac{0.186(10)}{0.447(6)} = 416.$$

Hence, the approach from Table 12 seems to be superior.

In Ref. [5], the integrated singular basis method (ISBFM) and the integral method are used to seek the solutions of the traditional cracked beam problem, and their leading coefficients are listed in Table 17 with the number of significant digits. Evidently, the leading coefficients in Tables 13 and 15 have more significant digits than those in Table 17.

In this paper, the same S is chosen for both Motz's and the cracked beam problems, in order to unify the theoretical frame work and to do comparisons. Let us look at the coefficients in Tables 5 and 12. The coefficients D_i decease monotonically in magnitude as $i \to \infty$, but $\hat{D}_\ell$ do not. However, each of $\hat{D}_{4\ell}$ and $\hat{D}_{4\ell+1}$ does decrease monotonically. We have carefully checked the coefficients from Tables 5, 12 and Refs. [15,22] to find the following empirical asymptotes

$$D_i \le C_0 \times 2.04^{-i}, \quad \hat{D}_{4\ell} \le C_1 \times 2.05^{-4\ell}, \quad \hat{D}_{4\ell+1} \le C_2 \times 2.01^{-4\ell-1}, \tag{5.15}$$

Table 17
The leading coefficients α_i cited from Georgiou, Boudouvis and Poullikkas (1997) [5] directly from the traditional cracked beam problem in Fig. 3

i	ISBFM	Number of significant	Integrated method	Num of significant
0	0.191118631972	12	0.191118631972	12
1	−0.1181160720	10	−0.118116071967	12
4	−0.1254698598(−1)	10	−0.1254698598(−1)	10
5	−0.1903340371(−1)	10	−0.1903340371(−1)	10
8	−0.6541248(−3)	7	−0.654125(−3)	6
9	−0.75959348(−2)	8	−0.7595935(−2)	7
12	−0.505411(−3)	6	−0.5054(−3)	4
13	−0.4477115(−2)	7	−0.44771(−2)	5
16	−0.190964(−3)	5	−0.19(−3)	2
17	−0.300990(−2)	6	−0.301(−2)	3
20	−0.1179(−3)	4	NA	/
21	−0.22019(−2)	5	NA	/
24	−0.72(−4)	2	NA	/

In the table 'NA' denotes 'not available'.

where C_0, C_1 and C_2 are positive constants. Hence, we may assume the true coefficients d_i in Eq. (1.4) also satisfy the same asymptotes

$$d_i \le C(2+\epsilon)^{-i}, \tag{5.16}$$

where ϵ is a small positive constant. Rewrite Eq. (1.4) as the sum of

$$\bar{u}_N = \sum_{i=0}^{N} d_i r^{i+(1/2)} \cos\left(i+\frac{1}{2}\right)\theta, \tag{5.17}$$

and the remainder

$$R_N = \sum_{i=N+1}^{\infty} d_i r^{i+(1/2)} \cos\left(i+\frac{1}{2}\right)\theta. \tag{5.18}$$

Below, we show the following exponential convergence

$$\|u-\bar{u}_N\|_{1,S} = \|R_N\|_{1,S} \le C_3\left(\frac{\sqrt{2}}{2}\right)^N, \tag{5.19}$$

where C_3 is a constant independent of N.

Denote a half-disk domain $S_R = \{(r,\theta)|0 \le r \le R, 0 \le \theta \le \pi\}$. Then $S \subset S_{\sqrt{2}}$. We have

$$\|R_N\|^2_{1,S} \le \|R_N\|^2_{1,S_{\sqrt{2}}} \tag{5.20}$$

$$= \int_0^{\pi}\int_0^{\sqrt{2}} \left\{\left(\frac{\partial R_N}{\partial r}\right)^2 + \frac{1}{r^2}\left(\frac{\partial R_N}{\partial \theta}\right)^2 + R_N^2\right\} r\,\mathrm{d}r\,\mathrm{d}\theta, \tag{5.21}$$

where

$$\frac{\partial R_N}{\partial r} = \sum_{i=N+1}^{\infty} d_i\left(i+\frac{1}{2}\right) r^{i-(1/2)} \cos\left(i+\frac{1}{2}\right)\theta, \tag{5.22}$$

$$\frac{1}{r}\frac{R_N}{\partial\theta} = -\sum_{i=N+1}^{\infty} d_i\left(i+\frac{1}{2}\right) r^{i-(1/2)} \sin\left(i+\frac{1}{2}\right)\theta. \tag{5.23}$$

By using the orthogonality of trigonometric functions, we obtain

$$I_1 = \int_0^{\pi}\int_0^{R}\left(\frac{\partial R_N}{\partial r}\right)^2 r\,\mathrm{d}r\,\mathrm{d}\theta = \frac{\pi}{4} R \sum_{i=N+1}^{\infty}\left(i+\frac{1}{2}\right) R^{2i} d_i^2, \tag{5.24}$$

$$I_2 = \int_0^{\pi}\int_0^{R}\frac{1}{r^2}\left(\frac{\partial R_N}{\partial \theta}\right)^2 r\,\mathrm{d}r\,\mathrm{d}\theta = \frac{\pi}{4} R \sum_{i=N+1}^{\infty}\left(i+\frac{1}{2}\right) R^{2i} d_i^2, \tag{5.25}$$

$$I_3 = \int_0^{\pi}\int_0^{R} R_N^2 r\,\mathrm{d}r\,\mathrm{d}\theta = \frac{\pi}{4}\sum_{i=N+1}^{\infty}\frac{1}{i+\frac{3}{2}} R^{2i+3} d_i^2 \le \frac{\pi R^3}{4}\sum_{i=N+1}^{\infty}\left(i+\frac{1}{2}\right) R^{2i} d_i^2. \tag{5.26}$$

Then, we have

$$\|R_N\|^2_{1,S} \le (I_1+I_2+I_3)|_{R=\sqrt{2}} \le \sqrt{2}\pi \sum_{i=N+1}^{\infty}\left(i+\frac{1}{2}\right)\sqrt{2}^{2i} d_i^2. \tag{5.27}$$

Under Eq. (5.16), we have

$$\|R_N\|^2_{1,S} \le C\sum_{i=N+1}^{\infty}\left(i+\frac{1}{2}\right)\left(\frac{\sqrt{2}}{2+\epsilon}\right)^{2i}. \tag{5.28}$$

From calculus, for $d = \sqrt{2}/(2+\epsilon) < 1$

$$\sum_{i=N+1}^{\infty}\left(i+\frac{1}{2}\right) d^{2i} \le C_1 N d^{2N} \le C_3\left(\frac{\sqrt{2}}{2}\right)^{2N}, \tag{5.29}$$

where C_3 is a constant independent of N. Combining Eqs. (5.28) and (5.29) gives the desired result (5.19).

Under Eq. (5.16), the exponential convergence rates in the infinite norm $\|\cdot\|_{1,\infty}$ and $\|\cdot\|_B$ can be proven similarly

$$\|u-\bar{u}_N\|_{1,\infty} = \|R_N\|_{1,\infty} \le C_4\left(\frac{\sqrt{2}}{2}\right)^N, \tag{5.30}$$

$$\|u-\bar{u}_N\|_B = \|R_N\|_B \le C_5\left(\frac{\sqrt{2}}{2}\right)^N, \tag{5.31}$$

where C_4 and C_5 are also positive constants. Then from Eqs. (3.7), (3.18) and (5.31) we have

$$\|u-\tilde{u}_N\|_B \le C\|u-\bar{u}_N\|_B \le C\|R_N\|_B \le CC_5\left(\frac{\sqrt{2}}{2}\right)^N, \tag{5.32}$$

and from Theorem 3.1

$$\|u-\bar{u}_N\|_1 \le C\left(\frac{\sqrt{2}}{2}\right)^N. \tag{5.33}$$

For the cracked beam in Fig. 2, the same exponential convergence rates hold as Eqs. (5.19), (5.30) and (5.31). The numerical rates $O(0.56^N)$ in Eqs. (4.8) and (4.9) are coincident with the a posteriori estimates $O(0.707^N)$. For the traditional scaled cracked beam in Fig. 3, the coefficients in Table 13 have

$$\alpha_i \le C\left(\frac{2}{2+\epsilon}\right)^i. \tag{5.34}$$

By noting that $\rho \le \sqrt{2}$, the same exponential convergence rates as Eqs. (5.19), (5.30) and (5.31) can also be obtained.

For the Laplace equations on sectors of disks, half-disks and disks, the exponential convergence rates of the expansion solutions are proven theoretically in Ref. [23, p. 41]. The proof for the exponential rates on the rectangular domains in S and $\hat{S}$ is given in this section by the a posteriori analysis, where the assumption (5.16) is purely based on numerical observation of the obtained results. For the rigorous proof of exponential convergence rates on S without Eq. (5.16) needs to be further explored.

6. Concluding remarks

To close this paper, let us make a few remarks.

1. Computational algorithms of the collocation Trefftz method are provided in Section 2. The overdetermined system (2.28) is recommended in computation since its algorithm is simple and easy, which is, indeed, just the collocation method at the boundary nodes, based on Proposition 2.1. The remarkable advantage of Eq. (2.28) is that the condition numbers of the associated matrix can be dramatically reduced, compared to Eq. (2.37) of the normal equation.
2. Different quadratures, such as the central and Gaussian rules, are investigated for the LSM. Theorem 3.1 reveals that different integration rules do not make much differences in the global errors over the entire domain S. However, the rules used may affect significantly the accuracy of the leading coefficient, based on numerical experiments in this paper.
3. The quadrature is used to link the collocation method and the LSM. However, from our error analysis, the accuracy of a quadrature may be very rough, in the sense that its relative errors are less than three quarters! This feature is significantly different from the traditional integral approximation in error analysis, e.g. the FEM analysis, where the integration errors should be chosen to balance the optimal errors of the solutions. Based on the analysis in Section 3, the solutions of Motz's and the cracked beam problems solved by the collocation Trefftz method have the exponential convergence rates. Note that Theorem 3.1 and Proposition 3.1 are new, which provide a theoretical foundation for high accuracy of the collocation Trefftz method (e.g. the BAM). This is also a justification for the collocation Trefftz method to become the most accurate method for Motz's and the cracked beam problems. Besides, the collocation methods both in S and on ∂S are explored in Ref. [8].
4. The numerical results in Section 2 are better than those in Refs. [14,16]. The Gaussian rule with six nodes are used to raise the accuracy of the leading coefficient to

   $$D_0 = 401.162453745234416 \tag{6.1}$$

   by the collocation Trefftz method. Compared with the more accurate value of D_0 in Refs. [14,15], this D_0 has exactly 17 significant digits, which error happens to coincide with the rounding errors of double precision. Note that coefficient D_0 in Ref. [16] has only 12 significant digits. This new discovery will change the evaluation of the BAM (i.e. the collocation Trefftz method) given in Ref. [14]. Based on the numerical results in Ref. [16] using the central rule, it is pointed out in Ref. [14, p. 133] that "BAM may produce the best global solutions", but "the conformal transformation method is the highly accurate method for leading coefficients". Now we may address that for Motz's problem, the collocation Trefftz method (i.e. the BAM) by the Gaussian rule of high order is a highly accurate method, not only for the global solutions but also for the leading coefficient D_0.
5. The new numerical results by the collocation Trefftz method in Section 4 provide a highly accurate solution for the cracked beam problem. The Gaussian rules of high order are used to raise the accuracy of the leading coefficient to

   $$\hat{D}_0 = 540.56512271362749, \tag{6.2}$$

   which also has 17 significant digits. For the traditional cracked beam problems in Fig. 3, coefficients

   $$\alpha_0 = 0.19111863197187209 \text{ and } \alpha_1 = -0.1181160719665095 \tag{6.3}$$

   from Table 13 have 17 and 16 significant digits, respectively. Thus the collocation Trefftz method using the Gaussian rule of high order is also a highly accurate method for the cracked beam problem, not only for the global solutions but also for the leading coefficient $\tilde{D}_0$.
6. Motz's and the cracked beam problems are linked and compared by considering the same domain S. The traditional crack model in Refs. [4–6,19,21] is formulated as a special case of the scaled cracked beam problem in this paper, whose solutions can be obtained straightforward by Eq. (5.5). Besides, numerical experiments from the approaches by Table 12 using Eq. (5.5) and by direct computation for Fig. 3 have been reported. The former seems to be superior due to its smaller condition numbers. Motz's and the cracked beam problems are regarded as the Laplace equations on S with two different boundary conditions along the edges.

Hence, different boundary conditions on ∂S may have different impacts on the singular behavior of the Laplace solutions in S. These computational results will appear later.

7. There was a special issue on the Trefftz methods, i.e. Advanced in Engineering Software, vol. 24, 1995. Some overviews can be found in Refs. [9,11,24]. In Refs. [9, 11], the Trefftz methods are classified into the indirect and direct methods. The collocation Trefftz in this paper is just the indirect Trefftz method. We use the same terminology, the Trefftz collocation method, as in Ref. [13]. The direct Trefftz method is analogous to the boundary element method except the fundamental functions are replaced by the singular function in the trial space. We report in this paper the new computational results and the new analysis of the indirect Trefftz method. In some extent, we have filled up the gap existing before between excellent computation and theoretical analysis of this method [10].

Acknowledgements

We are grateful to Prof. Alexander H.-D. Cheng for valuable communication, and also appreciate the reviewers for their very valuable comments and suggestions.

References

[1] Atkinson KE. An introduction to numerical analysis, 2nd ed. New York: Wiley; 1989. p. 276.
[2] Ciarlet PG. Basic error estimates for elliptic problems. In: Ciarlet PG, Lions JL, editors. Finite element methods (Part I). Amsterdam: North-Holland; 1991. p. 17–352.
[3] Demmel JW. Applied numerical linear algebra. Philadelphia: SIAM; 1997. p. 132.
[4] Fix GJ, Gulati S, Wakoff GI. On the use of singular functions with finite element approximations. J Comput Phys 1973;13:209–38.
[5] Georgiou GC, Boudouvis A, Poullikkas A. Comparison of two methods for the computation of singular solution in elliptic problem. J Comput Appl Math 1997;79:277–89.
[6] Georgiou GC, Olson L, Smyrlis G. A singular function boundary integral method for Laplace equation. Commun Numer Meth Eng 1996;12:127–34.
[7] Gloub GH, van Loan CE. Matrix computation, 2nd ed. Baltimore, MD: Johns Hopkins University Press; 1989.
[8] Hu HY, Li ZC. Collocation methods for Poisson's equations. Technical report. Department of Applied Mathematics, National Sun Yat-sen University, Taiwan; 2003.
[9] Jin JG, Cheung YK. Trefftz direct method. Adv Eng Software 1995; 24:65–9.
[10] Kamiya N, Kita E. Trefftz method 70 years. Adv Eng Software 1995; 24:1.
[11] Kita E, Kamiya N. Trefftz method: an overview. Adv Eng Software 1995;24:3–12.
[12] Lefeber D. Solving problems with singularities using boundary elements. Southampton: Computational Mechanics Publications; 1989.
[13] Leitao VMA. Applications of multi-region Trefftz-collocation to fracture mechanics. Eng Anal Bound Elem 1998;22:251–6.
[14] Li ZC. Combined methods for elliptic equations with singularities, interfaces and infinities. Boston: Kluwer Academic Publishers; 1998.
[15] Li ZC, Lu TT. Singularities and treatments of elliptic boundary problem. Math Comput Model 2000;31:97–145.
[16] Li ZC, Mathon R, Sermer P. Boundary methods for solving elliptic problems with singularity and interfaces. SIAM J Numer Anal 1987; 24:487–98.
[17] Lucas TR, Oh HH. The method of auxiliary mapping for the finite element solutions of elliptic problems containing singularities. J Comput Phys 1993;108(2):327–42.
[18] Motz M. The treatment of singularities of partial differential equations by relaxation methods. Q Appl Math 1947;4:371–7.
[19] Olson LG, Georgiou GC, Schultz WW. An efficient finite element method for treating singularity in Laplace's equation. J Comput Phys 1991;96:391–410.
[20] Rosser JB, Papamichael N. A power series solution of a harmonic mixed boundary value problem. Technical summary report #1405. University of Wisconsin, Madison Mathematics Research Center; 1975.
[21] Strang G, Fix GJ. An analysis of the finite element method. Englewood Cliffs, NJ: Prentice-Hall; 1973.
[22] Tang LT. Cracked-beam and related singularity problems. Master Thesis. Department of Applied Mathematics,National Sun Yat-sen University, Kaohsiung; 2000.
[23] Volkov EA. Block method for solving the Laplace equation and for constructing conformal mappings. Boca Raton: CRC Press; 1994.
[24] Zielinski AP. On trial functions applied in the generalized Trefftz method. Adv Eng Software 1995;24:147–55.